Journal of Current Science and Technology, January-March 2026 Vol. 16 No. 1, Article 163

ISSN 2630-0656 (Online)

Cite this article: Noipan, S., & Wutticharoenmongkol, P. (2026). Encapsulation of cinnamic acid in cellulose acetate hybrid membranes via electrospinning and electrospraying: A preliminary study toward wound dressing applications. *Journal of Current Science and Technology*, *16*(1), Article 163. https://doi.org/10.59796/jcst.V16N1.2026.163

Journal of Current Science and Technology

Journal homepage: https://jcst.rsu.ac.th

Encapsulation of Cinnamic Acid in Cellulose Acetate Hybrid Membranes via Electrospinning and Electrospraying: A Preliminary Study Toward Wound Dressing Applications

Supphakrit Noipan, and Patcharaporn Wutticharoenmongkol*

Department of Chemical Engineering, Faculty of Engineering, Thammasat School of Engineering, Thammasat University, Pathum Thani 12120, Thailand

*Corresponding Author; E-mail: tpatchar@engr.tu.ac.th

Received 30 July 2025; Revised 14 September 2025; Accepted 26 September 2025; Published online 20 December 2025

Abstract

Cinnamic acid (CN) was encapsulated in electrospun cellulose acetate (CA) nanofibers and the electrosprayed CA microparticles. The hybrid membrane (HM) was fabricated as a three-layer sandwich structure composed of electrospun CN-loaded CA nanofibers as the outer layers and the electrosprayed CN-loaded CA microparticles as the inner layer. The effects of CA concentration, type of solvent, and addition of CN on the morphology and sizes of either the electrospun nanofibers or the electrosprayed microparticles were investigated. The preliminary potential for using HM as wound dressings was investigated by comparing it with the electrospun nanofibers membrane (FM) and the cast films (CF). The release characteristics of CN from each type of membrane were investigated through total immersion and diffusion using Franz cell methods. For both methods, FM and HM exhibited greater CN released than CF. However, HM allowed more convenient CN release than FM, which contained only nanofibers. The mechanical properties in terms of tensile strength, Young's modulus, and elongation at break of these membranes were investigated. The antioxidant activities of HM, as determined by the 1,1-diphenyl-2-picrylhydrazyl (DPPH) assay, was the highest among all membrane types. All membranes exhibited antibacterial activitie against *Staphylococcus aureus (S. aureus)*, but not against *Escherichia coli (E. coli)*. Interestingly, HM showed the highest antibacterial activity against *S. aureus*. FM and especially HM may be promising for future wound dressing applications.

Keywords**:** *cellulose acetate; cinnamic acid; drug delivery; electrospinning; electrospraying; membrane; wound dressing*

1. Introduction

Electrospinning and electrospraying are two related but distinct techniques used in the fabrication of ultra-fine fibers or particles with diameters ranging from nanometers to micrometers. Both techniques utilize an electric field to eject the polymer solution or polymer melt from the nozzle to form either continuous fibers or discrete droplets or particles. Electrospinning is primarily employed to produce continuous fibers, while electrospraying is used to generate droplets or particles. A high-voltage power supply, a syringe with a nozzle, and the collector are the main configurations for both techniques. A high-voltage is applied between the nozzle and the collector to create either charged jets of polymer solution or fine droplets or particles, which solidify during flight onto the collector (Doshi & Reneker, 1995).

Depending on the solution and processing parameters, it is possible to control the formation of stable elongated fiber jets or droplets. In terms of solution parameters, polymer solutions or melts with sufficient viscosity are required to produce continuous fibers in electrospinning, while the less viscous solutions are dominant in producing droplets or particles in electrospraying (Demir et al., 2002; Moreira et al., 2021). In terms of processing parameters, an electric field above the critical voltage

promotes stable fiber elongation, whereas a low electric field contributes to droplet formation (Shenoy et al., 2005). Each technique has unique advantages and applications depending on the desired purpose. Electrospun fibers are utilized in applications such as filtration, nanocomposite, drug delivery, and tissue engineering (Mirjalili & Zohoori, 2016). Electrospraying finds applications in fields such as coating, encapsulation, and drug delivery (Cetinkaya et al., 2021; Jayan et al., 2019; Li et al., 2025; Li et al., 2023). The hybridization of electrospinning and electrospraying, referred to as electrospinning-electrospraying hydrodynamic (EDH) co-jetting, combines the advantages of both processes. Nanofibers and nanoparticles can be collected together or separately to fabricate hybrid materials with outstanding properties (Ekaputra et al., 2008; Nasari et al., 2022; Parın et al., 2022; Yanilmaz et al., 2014). The electrospinning-electrospraying hybrid technique has gained attention in various fields, including catalysis (Seo et al., 2020), sensors (Mokhtari et al., 2016), composites for batteries (Yanilmaz et al., 2014), protective clothing (Vitchuli et al., 2011), tissue engineering (Ekaputra et al., 2008; Nasari et al., 2022), and drug delivery systems (Nikolaou & Krasia-Christoforou, 2018; Parın et al., 2022; Yu et al., 2024). For controlled release systems, the hybrid nanofiber-nanoparticle material offers outstanding properties, including the controlled release of drug molecules from the nanoparticles and the mechanical properties from the nanofibers.

Recently, electrospun nanofibers have drawn attention in wound dressing applications due to their high surface area-to-volume ratio and interconnected porous structure, which allows oxygen and moisture vapor to pass through while preventing contaminants from entering the wound (Liu et al., 2017). Cellulose acetate (CA), a synthetic material derived from cellulose, a natural polymer found in plant cell walls, is one of the interesting materials employed as a carrier for controlled drug release in wound dressings. CA dressings are non-adherent to the wound bed and capable of absorbing and retaining wound exudate, thereby promoting a moist wound environment (Samadian et al., 2020). The success of wound dressing development depends on the selection of both matrix materials and loaded bioactive compounds that possess antioxidant, antibacterial, and anti-inflammatory properties. Cinnamic acid (CN), a natural compound that is commonly found in plants, particularly in the bark of cinnamon trees, has been incorporated into wound dressings due to its antioxidant (Gryko et al., 2021), antimicrobial (Taofiq et al., 2019; Yilmaz et al., 2018), and anti-inflammatory properties (Diniz et al., 2019; Taofiq et al., 2019). The antioxidant activity of CN helps protect cells from oxidative stress, therefore preventing impairment of the healing process. CN inhibited the growth of *Escherichia coli*, *Proteus mirabilis*, *Enterococcus faecalis*, *Staphylococcus aureus* bacteria, and the yeast, *Candida albicans* (Taofiq et al., 2019), which reduced the infection of the wound. In addition, CN possesses anti-inflammatory properties by suppressing the production of inflammatory cytokines (Diniz et al., 2019).

The present work reveals the novelty of CN encapsulated in CA hybrid membranes (HM) prepared by electrospinning-electrospraying. The HM was fabricated as a three-layer sandwich structure composed of electrospun nanofibers for the outer layers and electrosprayed microparticles for the inner layer. The potential use of HM as wound dressings was investigated and compared with the electrospun nanofiber membrane and the cast films, in which the release characteristics of CN from these membranes, the mechanical properties, the weight loss and water swelling, the antioxidant activity, and the antibacterial activity were studied.

2. Objectives

To investigate the effect of solution parameters on the morphology and size of the electrospun fibers and electrosprayed microparticle of CN-loaded CA, to fabricate the hybrid membrane assembled from the electrospun fibers and electrosprayed microparticles, and to examine the possibility for use of the hybrid membrane in wound healing applications.

3. Experimental

3.1 Materials

CA (Mw = 100,000 Da; acetyl content = 39.8%; hydroxyl content = 3.6%) and CN were purchased from Acros Organics (USA). Acetone and acetonitrile were purchased from Labscan Asia (Thailand). *N*,*N*-dimethylacetamide (DMAc), anhydrous disodium hydrogen orthophosphate (Na_2HPO_4), and monosodium dihydrogen orthophosphate monohydrate ($NaH_2PO_4.H_2O$) were purchased from Carlo Erba (Italy). Pyridinium formate and 1,1-diphenyl-2-picrylhydrazyl (DPPH) were purchased from Sigma-Aldrich (USA). All chemicals were analytical grade and were used without further purification.

3.2 Fabrication of Hybrid Membranes via Electrospinning and Electrospraying

3.2.1 Effect of Solvent Type and Concentration of CA

CA solutions were prepared at 17% and 22% w/v in 3 types of solvent mixtures composed of acetone:DMAc at 2:1, 1:1, and 1:2 v/v. The as-prepared solutions were subjected to a high direct current potential using a Gamma High-Voltage Research ES30P-5W power supply by loading them into a syringe with a stainless-steel needle (diameter of 0.91 mm) as a nozzle. The applied voltage was 20 kV, and the collection distance between the electrodes was 15 cm. A rotating drum with a width of 25 cm and a diameter of 7.7 cm was used to collect the electrospun fibers or electrosprayed particles at a rotating speed of 100 rpm. In addition, CA solutions containing 20% w/w CN were prepared in the same solvent mixtures and electrospun or electrosprayed under the same conditions. Pyridinium formate, which had been reported to increase the electrospinnability of polymer solutions (Wutticharoenmongkol et al., 2005), was also added to the solutions. Kinematic viscosities of the as-prepared solutions were measured using a Canon-Fenske Routine viscometer (Number 450: with a constant kinematic viscosity of 2.351 cSt/s at 40°C).

3.2.2 Morphology of the Electrospun Nanofibers and Electrosprayed Microparticles

The morphology of the electrospun nanofibers and electrosprayed microparticles was observed using a JSM-5410LV JEOL scanning electron microscope (SEM). Prior to observation under SEM, the samples were coated with a thin layer of gold using the Polaron SC7640 coater. The diameters of nanofibers and microparticles were measured from SEM images using the ImageJ software (version 1.52). The average diameters of the nanofibers and microparticles, along with their standard deviation were calculated from at least 100 measurements.

3.2.3 Fabrication and Assembling of the Membranes

In this present work, three types of CN-loaded CA membranes, including the electrospun fiber membrane (FM), the hybrid membrane (HM), and the cast film (CF), were studied. For the FM, it was prepared by electrospinning a 17% w/v CA solution containing 20% w/w CN in 2:1 v/v acetone:DMAc for 10 h. Pyridinium formate was also added to the solution at 2% v/v.

HM was fabricated as a three-layer sandwich structure. The first layer was the nanofibers made by electrospinning a 17% w/v CA solution containing 20% w/w CN in 2:1 v/v acetone:DMAc. pyridinium formate was also added to the solution at 2% v/v. The electrospinning time for this layer was 2 h. Later, the second layer consisted of microparticles made by electrospraying a 17% w/v CA solution containing 20% w/w CN in 1:2 v/v acetone:DMAc, which were collected on top of the first layer. The electrospraying time for this layer was 6 h. Lastly, the third layer was the nanofibers, which were fabricated using the same conditions as the first layer. The schematic illustration of the HM is shown in Figure 1.

CF was fabricated using a solvent-casting technique from the 17% w/v CA solution containing 20% w/w CN in 2:1 v/v acetone:DMAc.

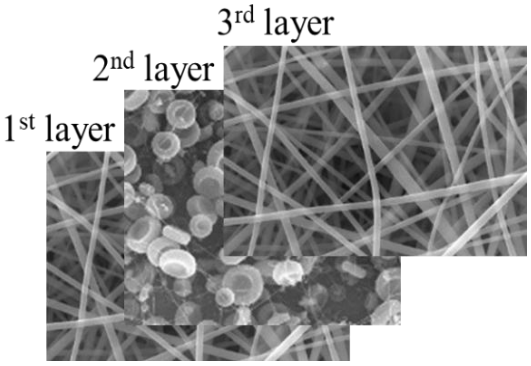

Figure 1 Schematic illustration of the three-layer hybrid membrane (HM)

3.3 Water Swelling and Weight Loss of the CA Membranes

The degree of water swelling and weight loss of each type of membrane (i.e., CF, FM, and HM) was examined after immersion in PBS at 37°C for 24 h. Each sample was cut into a square shape of 2x2 cm^2 and dried in an oven at 40°C for 4 h before immersion in PBS. The initial dry weight was recorded as M_i. At 24 h of immersion, the weight of the wet membrane was recorded as M. The membrane was then dried in an oven at 40°C for 8 h, and the dry weight after immersion was recorded as M_d. The percentages of water swelling and weight loss were calculated according to Equations (1) and (2), respectively.

$$\text{Water swelling (\%)} = \left(\frac{M - M_i}{M_i}\right) \times 100 \quad (1)$$

$$\text{Weight loss (\%)} = \left(\frac{M_i - M_d}{M_i}\right) \times 100 \quad (2)$$

3.4 Mechanical Properties of the CA Membranes

The mechanical properties of each type of membrane, including tensile strength, Young's modulus, and strain at break, were evaluated by the NRI Narin Instrument (Thailand) Universal Testing Machine according to the American Standard Testing Methods (ASTM-D882). The membranes, with an average thickness of about 80 ± 15 µm, were cut into rectangles of 10x90 mm^2 and tested under a load of 10 kN at 25°C. The crosshead speed and gauge length were 10 mm/min and 50 mm, respectively. At least five measurements were performed for each type of membrane.

3.5 Release of CN from the CA Membranes

3.5.1 Preparation of PBS

In the release study, phosphate buffer saline (PBS) was used as the releasing medium. For the preparation of 1 L of PBS, 3.4 g of $NaH_2PO_4.H_2O$ and 20.2 g of Na_2HPO_4 were dissolved in distilled water. The final volume was adjusted to 1 L. The pH of the obtained PBS was 7.4. A few drops of concentrated HCl or 1 M NaOH could be added to adjust pH.

3.5.2 Actual CN Content in the CA Membranes

Prior to studying the release of CN from the membranes, the actual amounts of CN in the membranes were quantified for use as the base values in the calculation of the percentage of release. Each type of membrane was cut into a square shape of 2x2 cm^2 and was completely dissolved in 100 mL of acetonitrile. Later, the absorbance of the solution was measured by a Shimadzu UV-1601 UV-Vis spectrophotometer at a wavelength of 273 nm (λ_{max}). The amounts of CN were quantified from the absorbances against the standard curve plotted between the concentrations of CN in acetonitrile and their absorbances at 273 nm.

3.5.3 Release Assay

The release characteristics of CN from the three types of CN-loaded CA membranes (i.e., CF, FM, and HM) were investigated by a total immersion method and a diffusion method using a Franz diffusion cell. The experiments were performed at 37°C using PBS (pH 7.4) as the releasing medium in order to simulate the physiological conditions for the proposed application as a wound dressing.

For the total immersion method, the tested membrane was cut into a square shape of 2x2 cm^2 and immersed in 40 mL of PBS. The medium was slowly stirred using a magnetic stirrer during the release time, ranging between 0-480 min. At each specified time point, 1.0 mL of releasing medium was collected and diluted with an appropriate amounts of PBS before measuring the absorbance at 273 nm. Meanwhile, 1.0 mL of the fresh PBS was refilled into the releasing bottle to maintain a constant volume of medium. The experiments were carried out in triplicate.

The amounts of CN released from the membranes were calculated from the absorbances against the standard curve plotted between the concentrations of CN in PBS and their absorbances at 273 nm. The cumulative percentage of CN released at each time point was calculated using an Equation (3):

$$\text{Cumulative CN release } (\%) = \frac{C_t}{C_{total}} \times 100 \qquad (3)$$

where C_t is the cumulative weight of CN released at time t and C_{total} is the actual initial weight of the CN in the membranes.

3.6 Antioxidant Activity of the CA Membranes

The antioxidant activities of three types of CN-loaded CA membranes (i.e., CF, FM, and HM) were tested by the radical-scavenging DPPH assay. The tested membrane was cut into a square shape of 2x2 cm^2 and immersed in 40 mL of PBS at 37°C for either 30 or 60 min. At a given time point, 1.0 mL of the releasing medium was withdrawn and mixed with 3.0 mL of a 0.5 mM DPPH solution in methanol. The solution was kept in the dark for 30 min before measuring the absorbance at 517 nm by a Shimadzu UV-1601 UV-Vis spectrophotometer. The control sample, which contained 1.0 mL of PBS and 3.0 mL of 0.5 mM DPPH solution, was prepared and kept in the same condition as the tested samples. The experiments were carried out in triplicate. The antioxidant activity was calculated according to an equation (4):

$$\text{Antioxidant activity } (\%) = \left(\frac{A_C - A_S}{A_C}\right) \times 100 \qquad (4)$$

where A_C is the absorbance of the control and A_S is the absorbance of the tested sample.

3.7 Antibacterial activity of the CA membranes

The antibacterial properties of three types of CN-loaded CA membranes (i.e., CF, FM, and HM) were evaluated by the agar disc diffusion method based on the Japanese Industrial Standard (JIS L1902) for woven and non-woven textiles. Each type of

membrane was cut into a square shape of 5x5 cm^2 and sterilized by UV irradiation for 60 min on each side of the membrane prior to placing it on a glass plate containing bacteria in agar. The testing bacteria were Gram-positive *Staphylococcus aureus* (*S. aureus*: ATCC 25923) and Gram-negative *Escherichia coli* (*E. coli*: ATCC 25922). The plates were incubated at 37°C for 18 h. The length of the inhibition zone, which included the diameter of the membrane, was measured using the Image J software (version 1.52). The negative and positive controls were filter papers saturated with distilled water and ethanol, respectively.

3.8 Statistical Analysis

All data were presented as mean ± standard deviation. At least 5 replicates were carried out in the mechanical studies and 3 replicates for the other experiments. A paired two sample for means: t-test was performed. A statistical difference between two sets of data was considered significant when $p < 0.05$.

4. Results and Discussion

4.1 Fabrication of Electrospun Nanofibers and Electrosprayed Microparticles

4.1.1 Effect of Solvent Type

The electrospinning and electrospraying of CA at concentrations of 17% and 22% without and with CN loading were compared when using three different solvent systems, including acetone:DMAc at 2:1, 1:1, and 1:2 v/v. Table 1 shows the selected SEM images of the obtained electrospun fibers or electrosprayed particles along with the viscosities of the solutions, the appearances, and the average diameters of either fibers or particles. When the acetone content in the 17% CA solutions decreased, the smooth, round fibers transitioned into beaded fibers and eventually to microparticles. Similarly, when the acetone content in the 22% CA solutions decreased, the smooth, round fibers obtained from the 2:1 and 1:1 acetone:DMAc systems formed beaded fibers and droplets in the 1:2 system. A similar trend was observed. The high content of acetone, which is a good solvent for CA, contributed to the formation of fibers, promoted fiber formation, whereas lower acetone content led to beaded fibers and particle formation. However, the use of acetone as a single solvent in electrospinning is not suitable due to its low dipole moment (2.85) and dielectric constant (20.7 at 25°C). Moreover, acetone is a highly volatile solvent, which leads to clogging of the polymer at the nozzle. DMAc, which possesses a high dipole moment (3.72) and dielectric constant (38.6 at 25°C) (Shcherbakov & Artemkina, 2013), can increase electrospinnability and reduce the solvent evaporation rate.

Overall, the viscosities of the solutions prepared with the 1:2 solvent ratio were higher than those prepared with the 1:1 and 2:1 ratios. A lower acetone content resulted in a higher viscosity of the solution. In electrospinning, the higher viscosity of the solution generally leads to the formation of fibers rather than beaded fibers or droplets (Moreira et al., 2021). However, the observations in this study contrasted with this trend because viscosity is not the only parameter to describe the electrospun fiber formation. The reason could be the fact that DMAc is the poor solvent of CA, leading to limited polymer-chain relaxation and, therefore, the formation of droplets or beaded fibers instead of smooth fibers.

Interestingly, microparticles with either a flattened disc shape or a biconcave shape were produced from the 17% CA solutions without and with CN loading from the solvent with a 1:2 ratio. The morphology of the microparticles is shown in Table 1 and Figure 2. This morphology was selected for incorporation into the HM in the next section. In conclusion, the CA electrospun nanofibers could be produced by using the solvent with a 2:1 ratio, whereas the CA electrosprayed microparticles could be produced by using the solvent with a 1:2 ratio.

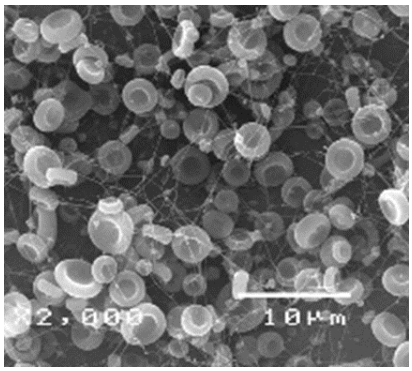

Figure 2 SEM images of round and biconcave CN-loaded CA microparticles prepared from 17% CA in 1:2 acetone:DMAc.

Table 1 SEM images, viscosities, and average diameters of CA nanofibers and microparticles with and without CN loading.

CA	CN	Acetone:DMAc 2:1	Acetone:DMAc 1:1	Acetone:DMAc 1:2
17%	Without CN	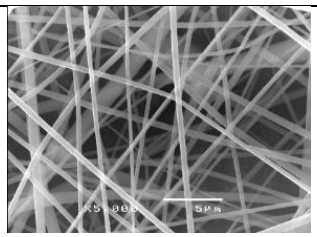 v = 509 ± 27 cSt/s Appearance: fibers ϕ = 441 ± 112 nm (fibers)	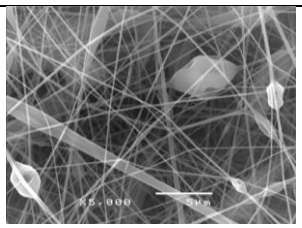 v = 581 ± 23 cSt/s Appearance: beaded fibers ϕ = 341 ± 298 nm (fibers)	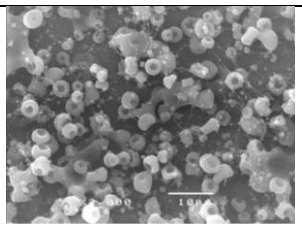 (*) v = 732 ± 20 cSt/s Appearance: micro-particles, droplets, and very small fibers ϕ = 3.48 ± 1.1 µm (particles)
	With CN	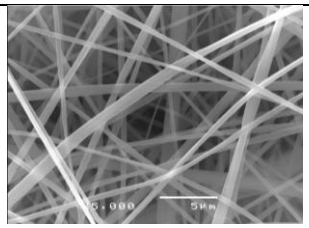 v = 563 ± 21 cSt/s Appearance: fibers ϕ = 561 ± 98 nm (fibers)	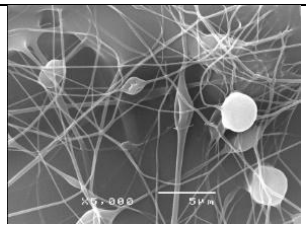 v = 621 ± 23 cSt/s Appearance: beaded fibers and droplets ϕ = 356 ± 312 nm (fibers)	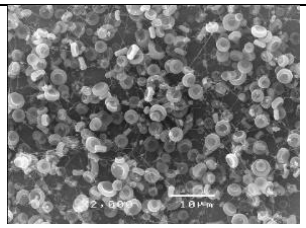 (*) v = 792 ± 19 cSt/s Appearance: micro-particles and very small fibers ϕ = 2.97 ± 0.41µm (particles)
22%	Without CN	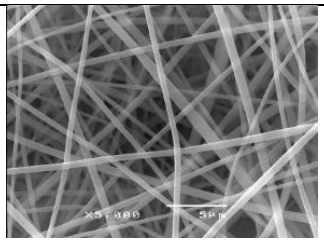 v = 534 ± 18 cSt/s Appearance: fibers ϕ = 522 ± 57 nm (fibers)	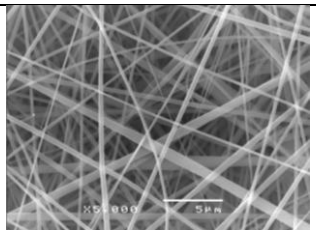 v = 587 ± 17 cSt/s Appearance: fibers ϕ = 454 ± 72 nm (fibers)	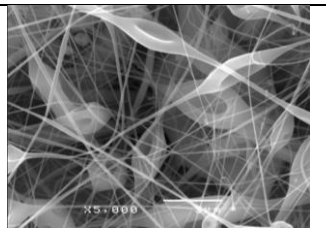 v = 852 ± 22 cSt/s Appearance: beaded fibers ϕ = N/A
	With CN	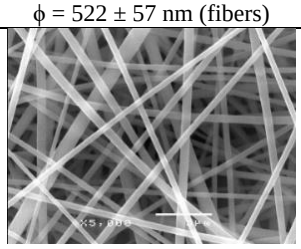 v = 572 ± 15 cSt/s Appearance: fibers ϕ = 594 ± 65 nm (fibers)	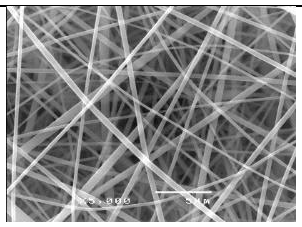 v = 585 ± 21 cSt/s Appearance: fibers ϕ = 465 ± 76 nm (fibers)	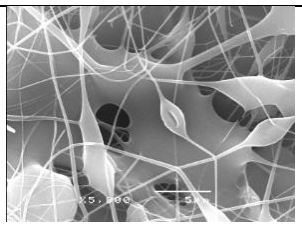 v = 863 ± 21 cSt/s Appearance: beaded fibers and droplets ϕ = N/A

Note: The magnification of images was x5000 except for (*) which was x2000.

Table 2 SEM images and average fiber diameters of electrospun CA nanofibers prepared with varying pyridinium formate concentrations.

Amounts of pyridinium formate (%)	**0**	**2**	**4**	**6**	**8**
SEM images	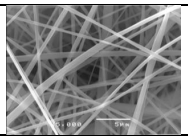	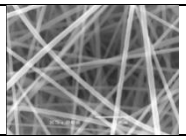	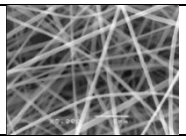	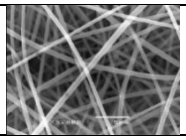	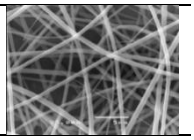
Averaged diameter of fibers (nm)	561 ± 98	568 ± 43	565 ± 51	563 ± 49	572 ± 47

4.1.2 Effect of Concentration of CA and Addition of CN

The effect of CA concentration on the morphology and size of nanofibers or microparticles was also investigated. For the solvent with a 2:1 ratio, the average fiber diameters increased when the CA concentration increased from 17% to 22%. Furthermore, the average fiber diameters increased upon CN loading for both the 17% and 22% CA solutions. The larger fiber size corresponded to the higher viscosities of the as-prepared solutions, which determine the greater viscoelastic force during electrospinning. The increased viscoelastic force resulting from greater polymer-chain entanglement opposes the stretching electrostatic and Coulombic forces, thereby contributing to larger fibers (Mit-uppatham et al., 2004; Moreira et al., 2021).

However, even though both the 17% and 22% CA solutions without and with CN loading provided the nanofibers, it should be noted that electrospinning the 22% CA solutions was more difficult than electrospinning the 17% CA solutions because the 22% CA solutions were more viscous and therefore more difficult to flow through the spinneret.

For the 1:1 solvent ratio, beaded nanofibers were obtained from the 17% CA solutions, whereas smooth-surfaced nanofibers were obtained from the 22% CA solutions. The higher viscosities of the 22% CA solutions contributed to the higher viscoelastic force, which reduced the formation of droplets or beaded fibers and allowed more fiber formation (Mit-uppatham et al., 2004; Moreira et al., 2021).

For the solvent with a 1:2 ratio, the round and biconcave shape microparticles were obtained from the 17% CA solutions, whereas the beaded nanofibers were obtained from the 22% CA solutions. The optimal CA concentration and suitable solvent system provided the production of the microparticles, which were employed in the fabrication of HM.

4.1.3 Effect of Addition of an Organic Salt

Pyridinium formate was added to the 17% CA solution with CN loading solutions in the solvent with a 2:1 ratio at concentrations of 2, 4, 6, and 8% v/v. Table 2 shows the SEM images of the obtained electrospun fibers and the average fiber diameters. The average fiber diameters from each condition were comparable and were in a range of 561–572 nm. It was found that the addition of pyridinium formate decreased the evaporation rate during the electrospinning process, preventing the solidification of polymer droplets at the nozzle tip and allowing the electrospinning process to proceed smoothly. Pyridinium formate was chosen in this work because it is a volatile organic salt that is miscible with CA solution. Several studies report that adding organic salt (e.g., pyridinium formate) to polymer solutions can improve electrospinnability and process stability (Neamnark et al., 2006; Wutticharoenmongkol et al., 2005). A previous study reported that pyridinium formate completely vaporizes during the electrospinning process, which was confirmed from the IR spectra of the electrospun fibers (Wutticharoenmongkol et al., 2005). Given the similar morphology and diameter of the electrospun fibers, pyridinium formate was added to the solutions at 2% v/v for the further fabrication of CA nanofibers for FM and HM.

4.2 Mechanical Properties of the CA Membranes

In the following sections, three types of CN-loaded CA membranes, including the cast films (CF), the fiber membrane (FM), and the hybrid membrane (HM), were fabricated. The nanofibers were fabricated from 17% CA in 2:1 v/v acetone:DMAc solution containing 20% w/w CN with 2% v/v pyridinium formate added, which was designated as FM and was also used as the outer layers of HM. The microparticles were prepared from 17% CA in 1:2 v/v acetone:DMAc solution containing 20% w/w CN for the inner layer of HM.

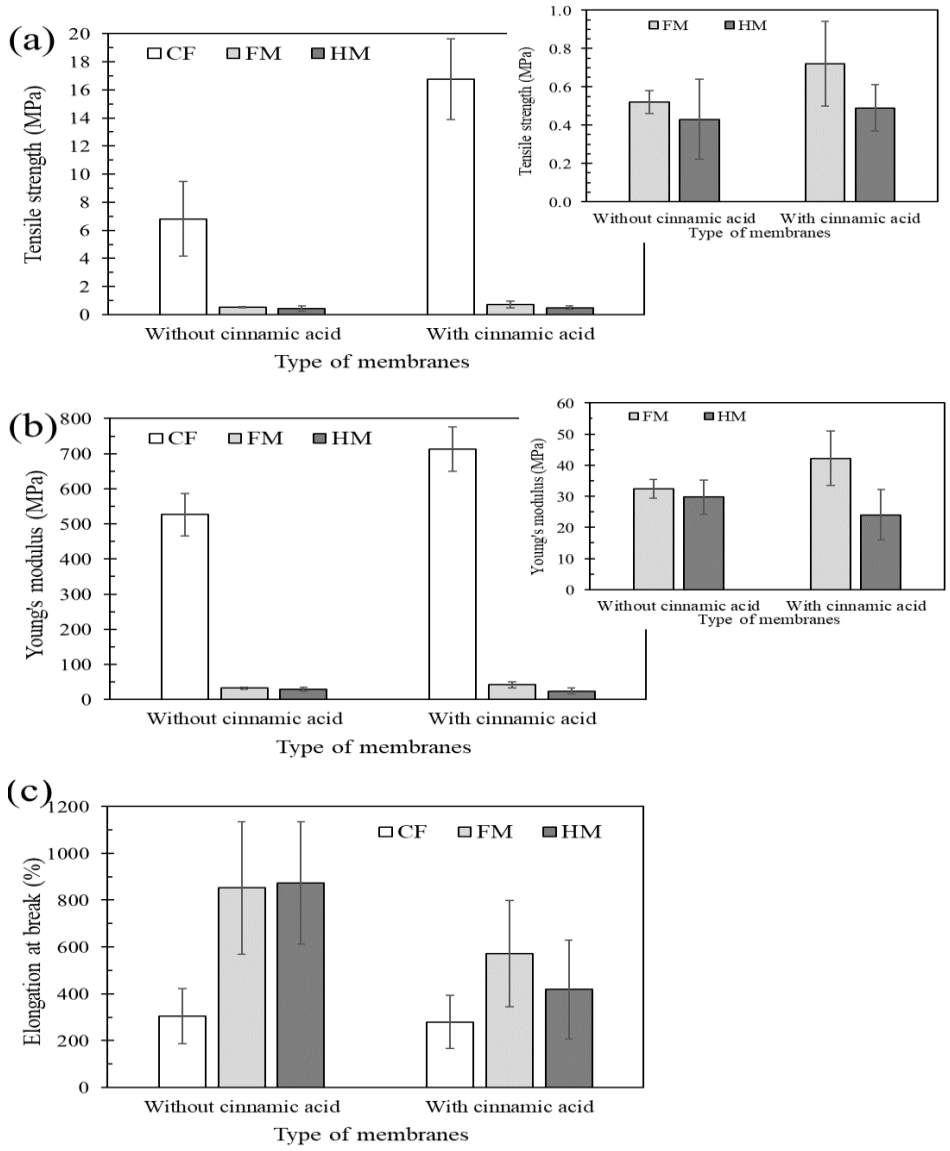

Figure 3 Mechanical properties of CF, FM, and HM with and without CN loading: (a) tensile strength, (b) Young's modulus, and (c) elongation at break

Figure 3 shows the mechanical properties, including tensile strength, Young's modulus, and elongation at break, of both the membranes with and without CN loading. The average thicknesses of CF, FM, and HM were about 95 ± 15, 62 ± 13, and 60 ± 15 µm, respectively. According to the dense structure and a higher thickness of CF, even though they were carefully prepared to be the thinnest as possible, it was found that much greater tensile strength and Young's modulus of CF were observed compared to those of FM and HM. In contrast, the elongations at break of CF were lower than those of FM and HM.

Comparing FM and HM for both without and with CN loading, it was found that the tensile strength, Young's modulus, and elongation at break of FM were higher than those of HM. Except for the elongation at break of the non-CN loading samples, their values were comparable. The discontinuous structure of the microparticles in the middle layer of HM likely contributed to the lower tensile strength and Young's modulus, as the material had a reduced ability to bear load. Additionally, the elongation at break of HM was lower than that of FM due to the less continuous fiber structure and the more discontinuous microparticle layer in HM.

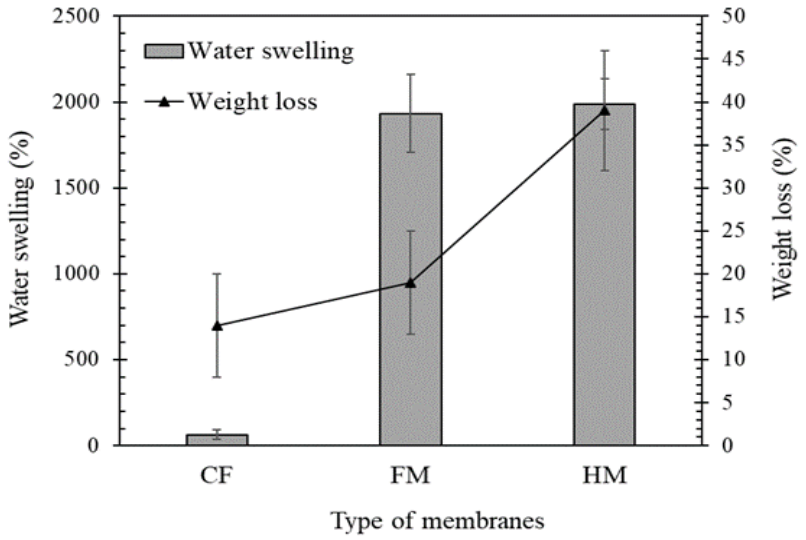

Figure 4 Water swelling and weight loss of the CN-loaded CF, FM, and HM at 24 h of immersion in PBS

The CN-loaded FM and HM possess sufficient mechanical strength for use as wound dressings. The elongation of CN-loaded FM and HM was about 420-570%, which was comparable to or even superior to that of the commercial wound dressings reported. Elongation of Kaltostat®, Aquacel Ag®, Exufiber®, Acticoat®, and Carbonet® was approximately 30-200%, while Mepilex®, Mepilex Ag®, Hydrosorb®, and Duoderm ET® were about 400-800%. Young's modulus of the CN-loaded FM and HM (about 24-42 MPa) was higher than those of the commercial wound dressings mentioned above (which were less than 7 MPa) except for Acticoat® (which was about 36 MPa). Similar to Young's modulus, the tensile strength of the CN-loaded FM and HM (approximately 0.4–0.7 MPa) was within a range comparable to that of commercial wound dressings except Acticoat® and Carbonet® (which were about 2.3-4.7 MPa) (Minsart et al., 2022).

4.3 Water Swelling and Weight Loss of the CA Membranes

Figure 4 illustrates the amounts of water swelling and weight loss of the CF, FM, and HM membranes at 24 h of immersion in PBS. The water swelling of FM and HM was approximately 1,933 ± 225%, whereas that of CF was about 64 ± 27%. The degrees of water swelling of FM and HM were similar and substantially greater than that of CF. Interconnected porous structures of fibers and microparticles in FM and HM provide a higher surface-area-to-volume ratio and inter-fibrous or inter-microparticle spaces for retaining water, leading to greater water swelling compared with CF, which has a dense structure (Opanasopit et al., 2008; Tungprapa et al., 2007; Wutticharoenmongkol et al., 2019).

Another important property of the wound dressing materials is the amount of weight loss, which is used to evaluate the stability of the mats and describe the release characteristics of drugs or active molecules. The weight loss of CF, FM, and HM was about 14 ± 6, 19 ± 6, and 39 ± 7%, respectively. The greater weight loss of FM compared with CF was due to its highly porous structure, which allowed more surface area to contact the medium. Interestingly, HM exhibited an even higher weight loss than FM. The microparticles in the middle layer of HM may have detached from the membrane during immersion, contributing to the higher weight loss. The amounts of swelling and weight loss are discussed along with the release study in the next section.

4.4 Release of CN from the Membranes

Prior to investigating the release profile of CN from the membranes, the standard curve of CN in PBS (pH 7.4) was constructed. The plot of CN concentrations in PBS versus their absorbance at 273 nm was a straight line with the linear equation $y = 0.132x - 0.0066$. For this equation, y is the UV absorbance value, and x is the CN concentration in ppm or mg/L. The coefficient of determination (r^2), which indicates the goodness of fit, was 0.9999.

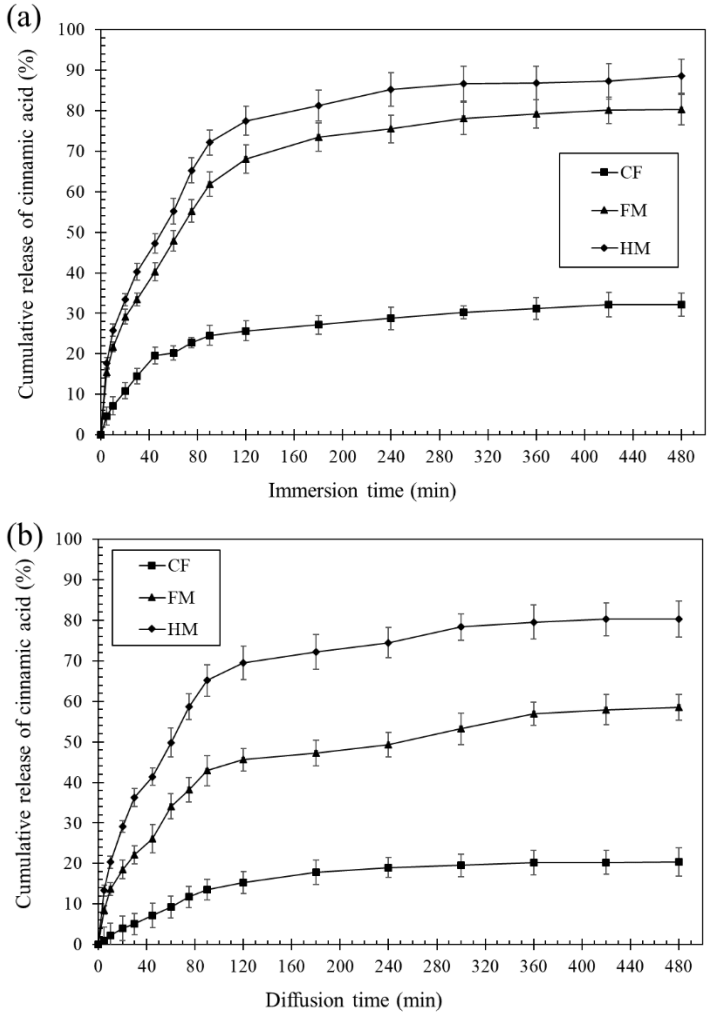

Figure 5 Cumulative release amounts of CN from the CN-loaded CF, FM, and HM from (a) total immersion and (b) diffusion through Franz cell methods in PBS (pH 7.4) at 37°C

4.4.1 Actual CN Content in the Membranes

Prior to calculating the release amounts of CN from the membranes, the actual CN contents in the membranes were evaluated for use as base values in the calculation of the release study. The percentage of actual CN content was obtained from the actual weight of CN presented in the membrane divided by the weight of the membrane. The average percentages of actual CN contents in CF, FM, and HM were 18.2 ± 1.3%, 16.8 ± 2.1, and 16.7 ± 2.3% respectively.

4.4.2 Release Characteristics of CN from the Membranes

The release of CN from CF, FM, and HM membranes was studied by total immersion and diffusion through Franz cell methods in PBS (pH 7.4) at 37°C for 480 min (8 h).

1) Release of CN by total Immersion Method

Figure 5a shows the percentages of cumulative CN released from these membranes by the total immersion method. The percentage of cumulative CN release was calculated from the cumulative weight of CN released divided by the actual amount of CN in the membrane.

It is evident that the amounts of CN released from FM and HM were much greater than those of CF at any given time point. The greater amounts of CN released from FM and HM than those from CF were due to the highly porous structures of FM and HM, which provided a higher surface area-to-volume ratio to allow more drug molecules to diffuse out of the matrix. The results of the release study were also well correlated with the degree of water swelling and weight loss, with HM being the highest, followed by

FM and CF, respectively. The higher degree of water swelling indicates that the membrane can hold more water or become more highly solvated, therefore facilitating the drug molecules to diffuse out conveniently (Opanasopit et al., 2008; Tungprapa et al., 2007; Wutticharoenmongkol et al., 2019).

For FM and HM, the burst release of CN was observed at the initial time of release. Specifically, two regions of the burst release were found in the first range of 0–10 min and the second range of 10-90 min, in which the release rate was slower than during the first burst phase. The amounts of CN released from HM were greater than those from FM at any given time point. The percentages of CN released from FM and HM at 10 min were about 21.7 ± 1.2% and 25.8 ± 1.6%, respectively. Subsequently, the percentages of CN released from FM and HM at 90 min were about 61.9 ± 3.1% and 72.1 ± 3.1%, respectively. Later, the gradual release of CN was observed since 90 min from both FM and HM until reaching a plateau in which the maximum percentages of CN released at 480 min were approximately 80.2 ± 3.7% and 88.5 ± 4.2%, respectively. In contrast, the gradual release of CN from CF was observed since the beginning of the release. The maximum percentage of CN released at 480 min from CF was about 32.1 ± 2.9%.

Interestingly, it was found that CN was released from HM in greater amounts than from FM. The results indicate that CN could be more conveniently released from HM, which contains microparticles in the middle layer of the membrane. Based on the studies of the release and the mechanical properties, the results suggested that the electrosprayed microparticles bestowed the drug release, while the electrospun fibers contributed sufficient mechanical properties to the membrane.

2) Release of CN by Diffusion through Franz Cell Method

The release experiments were also performed by diffusion through the Franz cell method in order to simulate the actual conditions under which the wound dressings are utilized. The release profiles of CN from CF, FM, and HM are shown in Figure 5b. For each type of membrane, smaller amounts of CN were released compared to those from the total immersion method. The smaller contact area of the membrane with the medium in the case of diffusion through the Franz cell method provided fewer amounts of drug release than that in the case of the total immersion method.

Comparing among the three types of membranes, the same trend of CN released as that from the total immersion method was observed, in which HM exhibited the greatest percentages of CN released at any given time point, followed by FM and CF, respectively. CN was rapidly released from all types of membranes in the initial time of release and later gradually released until reaching constant values. The maximum percentages of CN released at 480 min from CF, FM, and HM were approximately 20.3 ± 3.5%, 58.5 ± 3.1%, and 80.3 ± 4.4%, respectively. The rate of release and the amounts of drug released in the medium depend on a number of factors, for example, the temperature of release (Aso et al., 1994), the solubility of drug in the releasing medium at a given pH (Sabzi et al., 2020), and the degree of swelling and the weight loss of a matrix (Lamoudi, Chaumeil et al. 2016). The greater amounts of CN released from FM and HM than those from CF were due to the higher water swelling and weight loss of FM and HM than those of CF as a result of their highly porous structures.

In comparison between FM and HM, the release profiles of CN were similar to those observed from the total immersion method, in which HM provided more amounts of CN released than FM at any given time point. Repeatedly, the results showed that both FM and HM facilitated a sustained release profile of CN. However, HM with the microparticles in the middle layer of membrane allowed more drug to be conveniently released than FM with only the nanofibers and suggested an enhanced efficiency of drug release compared to FM.

4.5 Antioxidant Activity of the CN-loaded CA Membranes

The antioxidant activities of the releasing medium of each type of CN-loaded CA membrane from the total immersion method at 30 and 60 min of releasing time were investigated by the DPPH assay. The decreasing in the absorbance of DPPH radical at 517 nm (λ_{max} of DPPH), resulting from the radical scavenging ability of CN was recorded and calculated to be the antioxidant activity using an equation (4). Figure 6 shows the antioxidant activities of the CN-loaded CF, FM, and HM at two different time points, including 30 and 60 min of immersion. Obviously, the antioxidant activity of HM was the highest at any time point. The values of FM were slightly lower than those for HM, while CF exhibited much lower antioxidant activities than those of FM and HM. The antioxidant activities correlated well with the release profiles, where HM revealed the highest percentages of release compared to those of FM and CF,

respectively, at any time point of release. The antioxidant activity of the CN-loaded FM and HM (about 25-34% at 60 min) was in a comparable range with other wound dressings prepared by hybrid systems. The diabetic wound dressing from the electrospun polycaprolactone/sulfated chitosan nanofibers and electrosprayed polydopamine nanoparticles exhibited approximately 31% and 33% DPPH removal at 60 min and 120 min, respectively (Sheng et al., 2022). This result also suggests the potential use of FM, and especially HM, as promising wound dressings.

4.6 Antibacterial Activity of the CN-loaded CA Membranes

One of the important properties of ideal wound-dressing materials is antibacterial activity. The antibacterial activities against *S. aureus* and *E. coli* bacteria of the CN-loaded CF, FM, and HM were tested by the agar disc diffusion method. The length of the inhibition zone produced by each type of membrane is shown in Table 3. Distilled water and ethanol were used as the negative and positive controls, respectively. It was found that none of the membranes inhibited the growth of *E. coli*. The results indicated that CN cannot inhibit the growth of *E. coli*. However, all membranes exhibited antibacterial activity against *S. aureus* that were observed in the large inhibition zone, which was even larger than that of ethanol as a positive control. This result was consistent with several previous studies that cinnamic acid showing antibacterial activity against *S. aureus* (Gram-positive) but not (or only weakly) against *E. coli* (Gram-negative) (Malheiro et al., 2019; Ruwizhi & Aderibigbe, 2020).

For *S. aureus* testing, among all types of membranes, HM produced the largest inhibition zone, followed by FM and CF, respectively. Repeatedly, these results agreed with the release profiles and the measurement of antioxidant activity, in which HM exhibited the greatest amounts of CN released and antioxidant activity, followed by those from FM and CF, respectively.

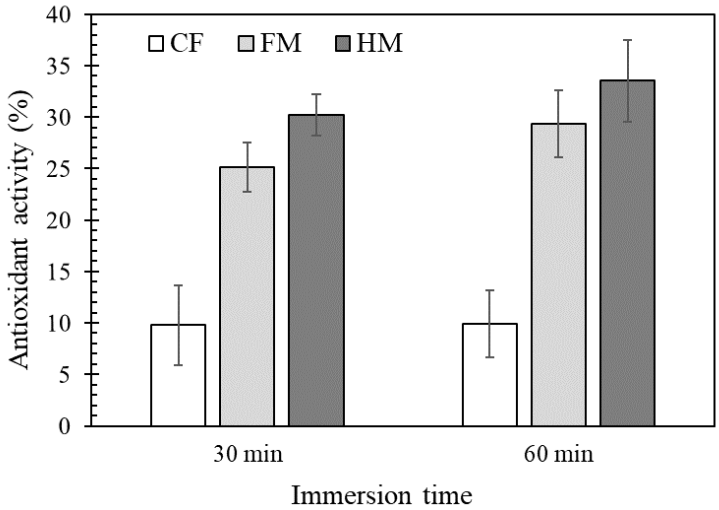

Figure 6 Antioxidant activities of the CN-loaded CF, FM, and HM at 30 min and 60 min of immersion.

Table 3 Antibacterial activity of CN-loaded CF, FM, and HM against *S. aureus* and *E. coli* determined by agar disc diffusion.

Sample	Length of inhibition zone (cm)	
	S. aureus	***E. coli***
Negative control (distilled water)	0.00 ± 0.00	0.00 ± 0.00
Positive control (ethanol)	6.20 ± 0.05	6.00 ± 0.05
CF	7.55 ± 0.25	0.00 ± 0.00
FM	8.20 ± 0.15	0.00 ± 0.00
HM	8.90 ± 0.30	0.00 ± 0.00

Based on the overall results, FM, and especially HM, demonstrated promising properties for use as wound dressings due to their sustained and high efficiency of drug release. In addition, they possess sufficient mechanical strength, antibacterial activity, and excellent antioxidant activity. Interestingly, HM exhibited greater CN release, higher antioxidant activity, and higher antibacterial activity against *S. aureus* than FM. However, this study has not yet investigated cytotoxicity and in vivo performance, which are critical properties for materials intended for wound dressing applications. This study primarily focuses on membrane fabrication and basic preliminary characterization. Therefore, the findings presented here should be considered as preliminary results that suggest the potential of these materials for future wound dressing applications. Further studies, including cytotoxicity and in vivo evaluations, are recommended to comprehensively assess their biomedical suitability.

5. Conclusions

In this study, hybrid membranes composed of cinnamic acid (CN)-loaded cellulose acetate (CA) were successfully fabricated. The electrosprayed CN-loaded CA microparticles were assembled in the middle layer, with electrospun nanofibers forming the outer layers. The use of the mixed solvent system of acetone:DMAc at 1:2 v/v facilitated the production of the electrosprayed microparticles, while the mixed solvent system at 2:1 v/v facilitated the formation of the electrospun nanofibers. The effects of concentration of CA, type of solvents, and addition of CN on the morphology and sizes of either the electrosprayed microparticles or electrospun fibers were investigated. The potential for use of HM as wound dressings was investigated by comparing it with the electrospun nanofiber membrane (FM) and the cast films (CF).

In the release study, HM, which contains microparticles in the middle layer of the membrane, allowed more CN to be more conveniently released than FM and CF, respectively, in both total immersion and diffusion Franz cell methods. The amounts of weight loss and water swelling of these membranes corresponded with the results of release. HM showed the highest antioxidant activity as determined by the DPPH assay, which was higher than FM and CF, respectively. All types of membranes exhibited antibacterial activities against *S. aureus* but not against *E. coli*. Consistently, HM showed the greatest antibacterial activity against *S. aureus*, followed by FM and CF, respectively.

Moreover, FM and HM possess sufficient mechanical strength. Even though their tensile strength and Young's modulus were not as good as those of CF, they were still considered promising materials for future wound dressing applications due to their high antioxidant and antibacterial activities. Especially, HM was more outstanding than FM due to the greater efficiency of CN release and superior antioxidant and antibacterial properties. However, the current study is considered as preliminary results that suggest the potential of these materials for future wound dressing applications. Other related evaluations, such as cytotoxicity and in vivo testing, are recommended for future studies.

6. Abbreviations

Abbreviation	Full Term
ASTM	American Standard Testing Methods
CA	Cellulose Acetate
CF	Cast Film
CN	Cinnamic Acid
DMAc	*N*,*N*-Dimethylacetamide
DPPH	1,1-Diphenyl-2-picrylhydrazyl
E. coli	*Escherichia coli*
EDH	Electrospinning–Electrospraying Hydrodynamic
FM	Electrospun Nanofiber Membrane
HM	Hybrid Membrane
JIS	Japanese Industrial Standard
PBS	Phosphate Buffer Saline
S. aureus	*Staphylococcus aureus*
SEM	Scanning Electron Microscope

7. CRediT Statement

Supphakrit Noipan: Methodology, Software, Investigation, Visualization.

Patcharaporn Wutticharoenmongkol: Conceptualization, Validation, Formal Analysis, Resources, Data Curation, Writing – Original Draft, Writing – Review & Editing, Visualization, Supervision, Project Administration, Funding Acquisition.

8. Acknowledgment

The authors acknowledge funding from the Faculty of Engineering, Thammasat School of Engineering, and the Research Unit in Polymer Rheology and Processing, Thammasat University.

9. References

Aso, Y., Yoshioka, S., Po, A. L. W., & Terao, T. (1994). Effect of temperature on mechanisms of drug release and matrix degradation of poly (d, l-lactide) microspheres. *Journal of Controlled Release*, *31*(1), 33-39. https://doi.org/10.1016/0168-3659(94)90248-8

Cetinkaya, T., Mendes, A. C., Jacobsen, C., Ceylan, Z., Chronakis, I. S., Bean, S. R., & García-Moreno, P. J. (2021). Development of kafirin-based nanocapsules by electrospraying for encapsulation of fish oil. *LWT*, *136*(2), Article 110297. https://doi.org/10.1016/j.lwt.2020.110297

Demir, M. M., Yilgor, I., Yilgor, E. E. A., & Erman, B. (2002). Electrospinning of polyurethane fibers. *Polymer*, *43*(11), 3303-3309. https://doi.org/10.1016/S0032-3861(02)00136-2

Diniz, L. R. L., Souza, M. T. D. S., Barboza, J. N., Almeida, R. N. D., & Sousa, D. P. D. (2019). Antidepressant potential of cinnamic acids: Mechanisms of action and perspectives in drug development. *Molecules*, *24*(24), Article 4469. https://doi.org/10.3390/molecules24244469

Doshi, J., & Reneker, D. H. (1995). Electrospinning process and applications of electrospun fibers. *Journal of Electrostatics*, *35*(2-3), 151-160. https://doi.org/10.1016/0304-3886(95)00041-8

Ekaputra, A. K., Prestwich, G. D., Cool, S. M., & Hutmacher, D. W. (2008). Combining electrospun scaffolds with electrosprayed hydrogels leads to three-dimensional cellularization of hybrid constructs. *Biomacromolecules*, *9*(8), 2097-2103. https://doi.org/10.1021/bm800565u

Gryko, K., Kalinowska, M., Ofman, P., Choińska, R., Świderski, G., Świsłocka, R., & Lewandowski, W. (2021). Natural cinnamic acid derivatives: A comprehensive study on structural, anti/pro-oxidant, and environmental impacts. *Materials*, *14*(20), Article 6098. https://doi.org/10.3390/ma14206098

Jayan, H., Leena, M. M., Sundari, S. S., Moses, J. A., & Anandharamakrishnan, C. (2019). Improvement of bioavailability for resveratrol through encapsulation in zein using electrospraying technique. *Journal of Functional Foods*, *57*, 417-424. https://doi.org/10.1016/j.jff.2019.04.007

Li, S., Yang, L., He, R., & Kong, L. (2025). Food-grade synthetic and natural polymers for electrospinning/electrospraying encapsulation of bioactive compounds. *Electrospinning and Electrospraying Encapsulation of Food Bioactive Compounds*, 53-61. https://doi.org/10.1016/B978-0-443-22228-3.00003-3

Li, X., Niu, X., Chen, Y., Yuan, K., He, W., Yang, S., ... & Yu, D. G. (2023). Electrospraying micro-nano structures on chitosan composite coatings for enhanced antibacterial effect. *Progress in Organic Coatings*, *174*, Article 107310. https://doi.org/10.1016/j.porgcoat.2022.107310

Liu, M., Duan, X. P., Li, Y. M., Yang, D. P., & Long, Y. Z. (2017). Electrospun nanofibers for wound healing. *Materials Science and Engineering: C*, *76*, 1413-1423. https://doi.org/10.1016/j.msec.2017.03.034

Malheiro, J. F., Maillard, J. Y., Borges, F., & Simões, M. (2019). Biocide potentiation using cinnamic phytochemicals and derivatives. *Molecules*, *24*(21), Article 3918. https://doi.org/10.3390/molecules24213918

Minsart, M., Van Vlierberghe, S., Dubruel, P., & Mignon, A. (2022). Commercial wound dressings for the treatment of exuding wounds: an in-depth physico-chemical comparative study. *Burns & Trauma*, *10*, Article tkac024. https://doi.org/10.1093/burnst/tkac024

Mirjalili, M., & Zohoori, S. (2016). Review for application of electrospinning and electrospun nanofibers technology in textile industry. *Journal of Nanostructure in Chemistry*, *6*(3), 207-213. https://doi.org/10.1007/s40097-016-0189-y

Mit-uppatham, C., Nithitanakul, M., & Supaphol, P. (2004). Ultrafine electrospun polyamide-6 fibers: Effect of solution conditions on morphology and average fiber diameter. *Macromolecular Chemistry and Physics*, *205*(17), 2327-2338. https://doi.org/10.1002/macp.200400225

Mokhtari, F., Latifi, M., & Shamshirsaz, M. (2016). Electrospinning/electrospray of polyvinylidene fluoride (PVDF): Piezoelectric nanofibers. *The Journal of The Textile Institute*, *107*(8), 1037-1055. https://doi.org/10.1080/00405000.2015.1083300

Moreira, A., Lawson, D., Onyekuru, L., Dziemidowicz, K., Angkawinitwong, U., Costa, P. F., ... & Williams, G. R. (2021). Protein encapsulation by electrospinning and electrospraying. *Journal of Controlled Release*, *329*, 1172-1197. https://doi.org/10.1016/j.jconrel.2020.10.046

Nasari, M., Poursharifi, N., Fakhrali, A., Banitaba, S. N., Mohammadi, S., & Semnani, D. (2023). Fabrication of novel PCL/PGS fibrous scaffold containing HA and GO through simultaneous electrospinning-electrospray technique. *International Journal of Polymeric Materials and Polymeric Biomaterials*, *72*(18), 1529-1545. https://doi.org/10.1080/00914037.2022.2112678

Neamnark, A., Rujiravanit, R., & Supaphol, P. (2006). Electrospinning of hexanoyl chitosan. *Carbohydrate Polymers*, *66*(3), 298-305. https://doi.org/10.1016/j.carbpol.2006.03.015

Nikolaou, M., & Krasia-Christoforou, T. (2018). Electrohydrodynamic methods for the development of pulmonary drug delivery systems. *European Journal of Pharmaceutical Sciences*, *113*, 29-40. https://doi.org/10.1016/j.ejps.2017.08.032

Opanasopit, P., Ruktanonchai, U., Suwantong, O., Panomsuk, S., Ngawhirunpat, T., Sittisombut, C., ... & Supaphol, P. (2008). Electrospun poly (vinyl alcohol) fiber mats as carriers for extracts from the fruit hull of mangosteen. *Journal of Cosmetic Science*, *59*(3), 233-242. https://doi.org/10.1111/j.1468-2494.2009.00462_5.x

Parın, F. N., Aydemir, Ç. İ., Taner, G., & Yıldırım, K. (2022). Co-electrospun-electrosprayed PVA/folic acid nanofibers for transdermal drug delivery: Preparation, characterization, and in vitro cytocompatibility. *Journal of Industrial Textiles*, *51*(1_suppl), 1323S-1347S. https://doi.org/10.1177/1528083721997185

Ruwizhi, N., & Aderibigbe, B. A. (2020). Cinnamic acid derivatives and their biological efficacy. *International Journal of Molecular Sciences*, *21*(16), Article 5712. https://doi.org/10.3390/ijms21165712

Sabzi, M., Afshari, M. J., Babaahmadi, M., & Shafagh, N. (2020). pH-dependent swelling and antibiotic release from citric acid crosslinked poly (vinyl alcohol)(PVA)/nano silver hydrogels. *Colloids and Surfaces B: Biointerfaces*, *188*, Article 110757. https://doi.org/10.1016/j.colsurfb.2019.110757

Samadian, H., Zamiri, S., Ehterami, A., Farzamfar, S., Vaez, A., Khastar, H., ... & Salehi, M. (2020). Electrospun cellulose acetate/gelatin nanofibrous wound dressing containing berberine for diabetic foot ulcer healing: In vitro and in vivo studies. *Scientific Reports*, *10*(1), Article 8312. https://doi.org/10.1038/s41598-020-65268-7

Seo, J. Y., Cho, K. Y., Lee, J. H., Lee, M. W., & Baek, K. Y. (2020). Continuous flow composite membrane catalysts for efficient decomposition of chemical warfare agent simulants. *ACS Applied Materials & Interfaces*, *12*(29), 32778-32787. https://doi.org/10.1021/acsami.0c08276

Shcherbakov, V. V., & Artemkina, Y. M. (2013). Dielectric properties of solvents and their limiting high-frequency conductivity. *Russian Journal of Physical Chemistry A*, *87*(6), 1048-1051. https://doi.org/10.1134/S0036024413060241

Sheng, Z., Xu, Y., Tong, Z., Mao, Z., & Zheng, Y. (2022). Dual functional electrospun nanofiber membrane with ROS scavenging and revascularization ability for diabetic wound healing. *Colloid and Interface Science Communications*, *48*, Article 100620. https://doi.org/10.1016/j.colcom.2022.100620

Shenoy, S. L., Bates, W. D., Frisch, H. L., & Wnek, G. E. (2005). Role of chain entanglements on fiber formation during electrospinning of polymer solutions: good solvent, non-specific polymer–polymer interaction limit. *Polymer*, *46*(10), 3372-3384. https://doi.org/10.1016/j.polymer.2005.03.011

Taofiq, O., Heleno, S. A., Calhelha, R. C., Fernandes, I. P., Alves, M. J., Barros, L., ... & Barreiro, M. F. (2019). Phenolic acids, cinnamic acid, and ergosterol as cosmeceutical ingredients: Stabilization by microencapsulation to ensure sustained bioactivity. *Microchemical Journal*, *147*, 469-477. https://doi.org/10.1016/j.microc.2019.03.059

Tungprapa, S., Jangchud, I., & Supaphol, P. (2007). Release characteristics of four model drugs from drug-loaded electrospun cellulose acetate fiber mats. *Polymer*, *48*(17), 5030-5041. https://doi.org/10.1016/j.polymer.2007.06.061

Vitchuli, N., Shi, Q., Nowak, J., Kay, K., Caldwell, J. M., Breidt, F., ... & Zhang, X. (2011). Multifunctional ZnO/Nylon 6 nanofiber mats by an electrospinning–electrospraying hybrid process for use in protective applications. *Science and Technology of Advanced Materials*, *12*(5), Article 055004. https://doi.org/10.1088/1468-6996/12/5/055004

Wutticharoenmongkol, P., Hannirojram, P., & Nuthong, P. (2019). Gallic acid-loaded electrospun cellulose acetate nanofibers as potential wound dressing materials. *Polymers for Advanced Technologies*, *30*(4), 1135-1147. https://doi.org/10.1002/pat.4547

Wutticharoenmongkol, P., Supaphol, P., Srikhirin, T., Kerdcharoen, T., & Osotchan, T. (2005). Electrospinning of polystyrene/poly (2-methoxy-5-(2′-ethylhexyloxy)-1, 4-phenylene vinylene) blends. *Journal of Polymer Science Part B: Polymer Physics*, *43*(14), 1881-1891. https://doi.org/10.1002/polb.20478

Yanilmaz, M., Lu, Y., Dirican, M., Fu, K., & Zhang, X. (2014). Nanoparticle-on-nanofiber hybrid membrane separators for lithium-ion batteries via combining electrospraying and electrospinning techniques. *Journal of Membrane Science*, *456*, 57-65. https://doi.org/10.1016/j.memsci.2014.01.022

Yilmaz, S. E. V. D. A. N., Sova, M., & Ergün, S. (2018). Antimicrobial activity of trans-cinnamic acid and commonly used antibiotics against important fish pathogens and nonpathogenic isolates. *Journal of Applied Microbiology*, *125*(6), 1714-1727. https://doi.org/10.1111/jam.14097

Yu, D. G., Gong, W., Zhou, J., Liu, Y., Zhu, Y., & Lu, X. (2024). Engineered shapes using electrohydrodynamic atomization for an improved drug delivery. *Wiley Interdisciplinary Reviews: Nanomedicine and Nanobiotechnology*, *16*(3), Article e1964. https://doi.org/10.1002/wnan.1964